

Interactions of velocity structures between large and small scales in microelectrokinetic turbulence

Wei Zhao^{1,*}, Weidong Su,² and Guiren Wang^{1,3}

¹State Key Laboratory of Photon-Technology in Western China Energy, International Scientific and Technological Cooperation Base of Photoelectric Technology and Functional Materials and Application, Institute of Photonics and Photon-technology, Northwest University, Xi'an 710127, China

²State Key Laboratory for Turbulence and Complex Systems, College of Engineering, Peking University, Beijing, China 100871

³Department of Mechanical Engineering & Biomedical Engineering Program, University of South Carolina, Columbia, South Carolina 29208, USA



(Received 13 April 2021; accepted 1 July 2021; published 22 July 2021)

Recent investigations on electrokinetic (EK) flows have indicated turbulentlike flow can be realized by applying strong and high frequency ac electric field to flows with high-conductivity-gradient interface, even though under low bulk flow Reynolds number. Relative to conventionally hydrodynamic turbulence in a high Reynolds number, the ac EK turbulent flow exhibits high randomness with stronger intermittency [Wang *et al.*, *Phys. Rev. E* **93**, 013106 (2016)]. The abnormally high intermittency could be attributed to the ascending probability density function of velocity gradients (dominated by small scale velocity structure function) far from the equilibrium state. By evaluating the intermittency of the ac EK turbulent flow with hierarchical structures, we astonishingly find the intermittency factor of hierarchical structures in SL94 law, i.e., β factor, which is commonly believed to be between 0 and 1, exhibits larger value than 1 in the ac EK turbulent flow. This result indicates the different hierarchical relations of flow structures in ac EK turbulence flow from that in the conventional hydrodynamic turbulence, as further illustrated by the probability density function of velocity structures among different spatial scales.

DOI: [10.1103/PhysRevFluids.6.074610](https://doi.org/10.1103/PhysRevFluids.6.074610)

I. INTRODUCTION

Turbulence is a complicated concept and normally, it is described as a spatial-temporal random flow which has a continuous kinetic energy cascade between large (integral scale) and small scale (e.g., Kolmogorov scale). To characterize the feature of multiscales, scaling laws of velocity structure functions are commonly used. Kolmogorov [1,2] advanced the classical self-similarity law of turbulence for high Reynolds number limit in 1941 as

$$S_p(l) = \langle |\Delta u(l)|^p \rangle \sim l^{\xi_p}, \quad (1)$$

where $\Delta u(l) = u(x+l) - u(x)$, $S_p(l)$ is the p^{th} moment of Δu on spatial scale l and ξ_p is the corresponding scaling exponent. The usage of the absolute value of $\Delta u(l)$ ensures that p can be taken as continuous real number usually being non-negative. By Kolmogorov's prediction $\xi_p = p/3$ should hold. However, it has been well known by a great deal of later experiments and numerical simulations that ξ_p is actually a nonlinear function with respect to p . Later, in 1962, Kolmogorov [3] advanced a refined similarity hypothesis which accounts for the influence of locally averaged

*Corresponding author: zwbayern@nwu.edu.cn

energy dissipation (ε_l), as $S_p(l) \sim \langle \varepsilon_l^p \rangle l^{\xi_p}$. By applying logarithmically normal distribution on energy dissipation, he found $\langle \varepsilon_l^p \rangle \sim l^{-\frac{\mu p}{18}(p-3)}$, and accordingly, $\xi_p = p/3 - \frac{\mu p}{18}(p-3)$ [1,4], with μ being an exponent. The departure of ξ_p from $p/3$ implies turbulence is intermittent for small length scales, accompanied with several aspects, such as the probability density function (PDF) of velocity increment departs from Gaussian distribution, etc. For 50 years, various phenomenological models were proposed to depict the intermittency with a more applicable scaling exponent function. In 1994, She and Leveque advanced a celebrated model [5] on the basis of hierarchical structures. In the following years, the SL94 model is supported by both experiments and numerical simulations, in hydrodynamic turbulence [6,7], thermal convection [8], and magnetohydrodynamic (MHD) turbulence [9], etc. The corresponding ξ_p in the SL94 model can be generally described by the three parameters directly as

$$\xi_p = \gamma p + C(1 - \beta^p), \quad (2)$$

where γ the scaling exponent of the most singular structures and C is the codimension. β is an intermittency factor which is crucial for describing the similarity of hierarchical structures, especially, it characterizes the intermittency of energy dissipation [10]. Normally $C > \gamma > 0$. In the original SL94 model, β is constant and $0 < \beta \leq 1$, which has also been supported by various reports [9,11,12].

II. THEORY

Nevertheless, a basic question arises: is β always limited to be within 0 and 1? Recall that the SL model implies a log-Poisson distribution of random multiplier connecting any pair of fluctuations at a small scale l and a large scale l_0 , respectively (see She and Waymire [4]). Based on this observation and thereafter by means of some techniques from probability theory, a rigorous relation can be derived linking the PDF of velocity increment at small scale and the one at large scale [13]. Let $P_l = P_l[\Delta u(l)]$, which represents the PDF of $\Delta u(l)$, then the relations between P_{l_0} and P_l can be expressed as

$$P_l = T_{l,l_0} \sum_{k=0}^{\infty} W_k P_{l_0} [\Omega_{l,l_0} \beta^{-k} \Delta u(l_0)], \quad (3)$$

where $W_k = (\beta^{-1} \ln M_{l,l_0})^k / k!$ is a weight function and

$$\begin{aligned} T_{l,l_0} &= l^{*C-\gamma} < 1 \\ \Omega_{l,l_0} &= l^{*-\gamma} > 1, \\ M_{l,l_0} &= l^{*-C} > 1 \end{aligned} \quad (4)$$

where $l^* = l/l_0$ is dimensionless length scale and $0 < l^* < 1$. Because Ref. [13] is not in English, we would like to comfort readers by indicating that from the PDF one can readily confirm by working with Eq. (3) that

$$\begin{aligned} S_p(l) &= \langle |\Delta u(l)|^p \rangle = \int |\Delta u(l)|^p P_l[\Delta u(l)] d\Delta u(l) \\ &= (l^*)^{\gamma p + C(1-\beta^p)} \int |\Delta u(l_0)|^p P_{l_0}[\Delta u(l_0)] d\Delta u(l_0) \\ &= (l^*)^{\gamma p + C(1-\beta^p)} S_p(l_0). \end{aligned} \quad (5)$$

Equation (3) could provide a potential way to expand β to a wider parameter space, e.g., $\beta > 1$, as follows. In conventional turbulence, where $0 < \beta \leq 1$, considering $C > \gamma > 0$, we have

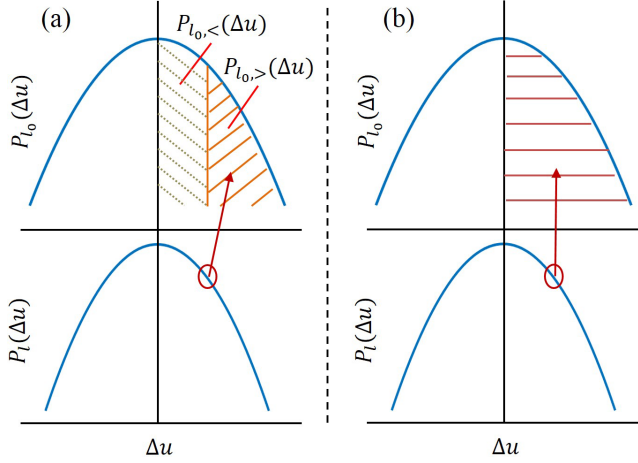


FIG. 1. Influence of β on the relation of P_l and P_{l_0} . (a) $0 < \beta \leq 1$, (b) $\beta > 1$.

$\Omega_{l,l_0}\beta^{-k} \geq 1$ for all k , thus

$$P_l = T_{l,l_0} \sum_{k=0}^{\infty} W_k P_{l_0, >}[\Delta u(l_0)], \quad (6)$$

where $P_{l_0, >}[\Delta u(l_0)] = P_{l_0}[\Delta u(l_0)]|_{\Delta u(l) \geq \Delta u(l_0)}$ and $P_{l_0, <}[\Delta u(l_0)] = P_{l_0}[\Delta u(l_0)]|_{\Delta u(l) < \Delta u(l_0)}$ denote the P_{l_0} at the higher and lower sides of $\Delta u(l_0)$, which is equal to $\Delta u(l)$, as diagrammed in Fig. 1(a). Equation (6) implies, in conventional turbulence, the PDF of $\Delta u(l)$ at small scales (for instance, marked by the red circle) is solely determined by the PDF of stronger velocity increments at large scales, i.e., $P_{l_0, >}[\Delta u(l_0)]$, as plotted by the green shadow region in Fig. 1(a). If $P_{l_0, >}[\Delta u(l_0)]$ is increased, P_l is increased too. Meanwhile, if l is significantly decreased, $\Omega_{l,l_0}\beta^{-k}$ can be much larger than unity. The PDF of $\Delta u(l)$ on small scale is tightly related to the small probability event of $\Delta u(l_0)$.

However, when $\beta > 1$, $\beta^{-k} < 1$ and $\Omega_{l,l_0} > 1$. There exists a $k_c = \ln \Omega_{l,l_0} / \ln \beta$ with

$$\begin{cases} \Omega_{l,l_0}\beta^{-k} > 1, & \text{for } 0 \leq k < k_c \\ \Omega_{l,l_0}\beta^{-k} < 1, & \text{for } k \geq k_c \end{cases}. \quad (7)$$

The PDF of $\Delta u(l)$ can be presented as

$$P_l = P_{l,1} + P_{l,2}, \quad (8)$$

where

$$P_{l,1} = T_{l,l_0} \sum_{k=0}^{k_c-1} W_k P_{l_0, >}[\Delta u(l_0)], \quad (9a)$$

$$P_{l,2} = T_{l,l_0} \sum_{k=k_c}^{\infty} W_k P_{l_0, <}[\Delta u(l_0)]. \quad (9b)$$

$P_{l_0, <}[\Delta u(l_0)]$ is plotted by the gray shadow region as diagrammed in Fig. 1(a). Compared to Eq. (6), in the calculation P_l of $\Delta u(l)$, both $P_{l_0, <}[\Delta u(l_0)]$ and $P_{l_0, >}[\Delta u(l_0)]$ must be taken into account, as can be seen in Eqs. (8), (9a), and (9b). Or in other words, both the high and low probability events of $\Delta u(l_0)$ have influence on the PDF of $\Delta u(l)$, as schematically plotted in Fig. 1(b). At large scales, the PDF of weak velocity increments could be much higher than that of strong counterparts, i.e., $P_{l_0, <}[\Delta u(l_0)] \gg P_{l_0, >}[\Delta u(l_0)]$. There also exists a k_w for weight function W_k . For $1 < k \leq k_w$, $W_k \geq$

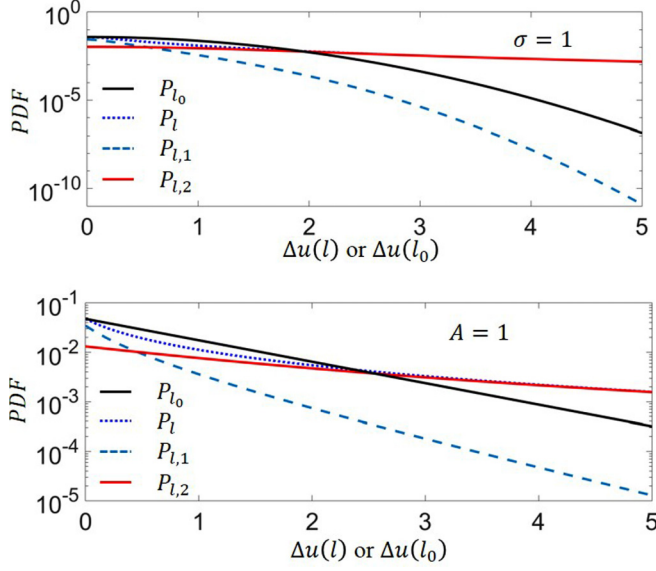


FIG. 2. Schematic of the relations between P_{l_0} and P_l at $l^* = 0.01$. Here, $C = 2$, $\beta = 3/2$, $\gamma = 2/3$. (a) P_{l_0} has Gaussian distributions with $\alpha_{l_0} = 1$, and (b) P_{l_0} has exponential decaying with $A = 1$.

1, while for $k > k_w$, $W_k < 1$. For the case $k_w \approx k_c$ (approximation relation is only for theoretical analysis and not true with high probability), even though $W_k < 1$, $W_k P_{l_0, <}[\Delta u(l_0)]$ can still be more important than $W_k P_{l_0, >}[\Delta u(l_0)]$. The overall contribution from $P_{l,2}$ can be non-neglectable. This may lead to abnormally high P_l at large $|\Delta u|$. The dependence of P_l on the large-scale counterpart P_{l_0} can be clearly distinguished from two symmetrical P_{l_0} which are typical in turbulence (asymmetry is not discussed here, even though it is commonly existed in turbulence). One is the Gaussian distribution

$$P_{l_0} = \frac{1}{\sigma_{l_0} \sqrt{2\pi}} \exp \left\{ -\frac{[\Delta u(l_0)]^2}{2\sigma_{l_0}^2} \right\}, \quad (10)$$

where σ_{l_0} is the standard derivation of $\Delta u(l_0)$. The other is exponential distribution to describe the influence of the exponential tail as a representation of strong intermittency in the following:

$$P_{l_0} = \frac{A}{2} \exp \{-A \Delta u(l_0)\}. \quad (11)$$

The results are plotted in Fig. 2, where $l^* = 0.01$, $C = 2$, $\beta = 3/2$, and $\gamma = 2/3$. From Fig. 2(a), when P_{l_0} has a Gaussian distribution which means weak intermittency, $P_{l,1}$ decreases faster than Gaussian distribution, as shown by the blue dashed line. In the region $\Delta u(l) \leq 0.6$, $P_{l,2} \leq P_{l,1}$, and P_l is dominated by $P_{l,1}$. While $\Delta u(l) > 0.6$, $P_{l,2} > P_{l,1}$. In this region, P_l is dominated by $P_{l,2}$ instead, with an approximately overlapping of P_l and $P_{l,2}$. When $\Delta u(l) > 1.8$, $P_{l,2}$ becomes even larger than P_{l_0} . The slowly decaying $P_{l,2}$ leads to a nearly exponential fall of P_l from the Gaussian distribution of P_{l_0} . It indicates, with $\beta > 1$, a turbulent flow without intermittency on large scale l_0 could become eventually intermittent on small scale l . Nevertheless, for P_{l_0} with exponential decay [Fig. 2(b)], P_l is dominated by $P_{l,2}$ when $\Delta u(l) > 0.5$. P_l also exhibits less steep than P_{l_0} . $P_l > P_{l_0}$ only emerges when $\Delta u(l) > 2.4$. We also find from Fig. 2 that at sufficiently large $\Delta u(l)$, P_l is always dominated by $P_{l,2}$ which leads to much flatter distributions.

Similar results can also be found at larger $l^* = 0.1$, with $C = 2$, $\beta = 3/2$, and $\gamma = 2/3$, as plotted in Fig. 3. As a result of the increasing l^* , the critical $\Delta u(l)$ where P_l becomes larger than P_{l_0} , are 1.9 (Gaussian) and 2.3 (exponential decay), respectively. P_l become dominated by $P_{l,2}$ when $\Delta u(l)$

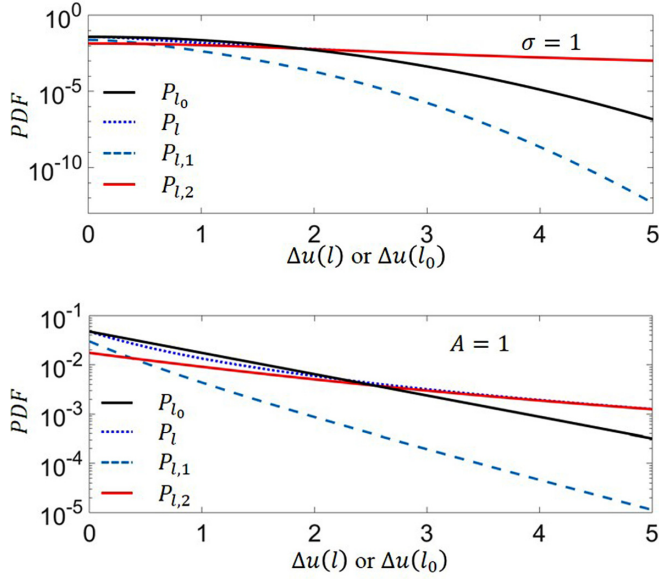


FIG. 3. Schematic of the relations between P_{l_0} and P_l at $l^* = 0.1$. Here, $C = 2$, $\beta = 3/2$, $\gamma = 2/3$. (a) P_{l_0} has Gaussian distributions, and (b) P_{l_0} has exponential decaying.

are over 0.5 (Gaussian) and 0.4 (exponential decay), respectively. The results for $l^* = 0.1$ and 0.01 indicate, when l^* is increased, $P_{l,2}$ becomes more important.

A direct comparison of $P_{l,2}$ for both Gaussian and exponential decay with cases of $l^* = 0.1$ and 0.01 are plotted in Fig. 4. With fixed C , β and γ in Fig. 4(a) are larger than those in Fig. 4(b),

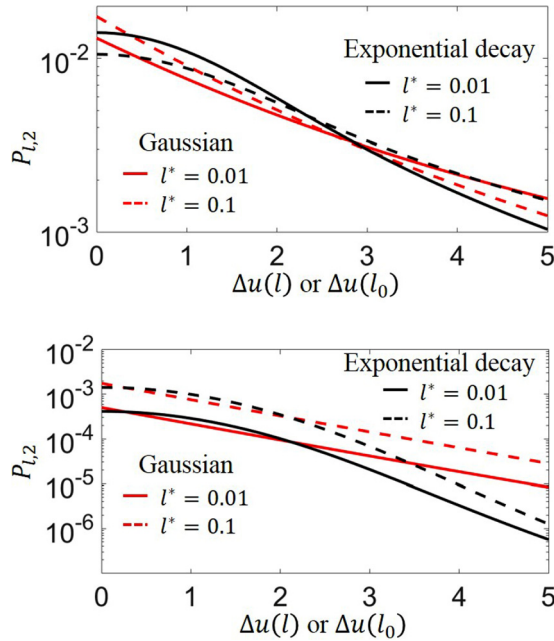


FIG. 4. $P_{l,2}$ calculated at different β and γ , when $C = 2$. (a) $\beta = 3/2$, $\gamma = 2/3$; (b) $\beta = 9/8$, $\gamma = 5/12$.

respectively. In Fig. 4(a), for the P_{l_0} of Gaussian distribution, as l^* is increased $P_{l,2}$ curves become steeper. This means, at smaller l^* , the small $\Delta u(l)$ components of P_{l_0} contribute more to the large $\Delta u(l)$ components of P_l through $P_{l,2}$. In contrast, for the P_{l_0} of exponential distribution, $P_{l,2}$ curves become less steep with increasing l^* . There exists a hump around $\Delta u(l) = 0$. At smaller l^* , the small $\Delta u(l)$ components of P_{l_0} contribute more to the small $\Delta u(l)$ components of P_l through $P_{l,2}$.

Unfortunately, these trends are not universal, but rely on β and γ . When β and γ are decreased to 9/8 and 5/12, respectively, as plotted in Fig. 4(b), the hump of $P_{l,2}$ for exponential decay becomes nonsignificant, and the $P_{l,2}$ curves becomes steeper with increasing l^* at the far end of $\Delta u(l)$. For the P_{l_0} of Gaussian distribution, $P_{l,2}$ curves are nearly parallel to each other.

By comparing Figs. 4(a) and 4(b), it can be seen that the increasing β and γ generally lead to (i) more contributions from $P_{l,2}$ and (ii) less steeper $P_{l,2}$ curves. Even for turbulent flows with P_{l_0} of the Gaussian distribution, i.e., no intermittency on a large scale, $P_{l,2}$ can still be non-negligible at large $\Delta u(l)$ on a small scale, or in other words, small scale intermittency. The intermittency of turbulent flow with higher β and γ is predictably stronger.

III. EXPERIMENTS

From the investigation above, it can be seen $\beta > 1$ is not strictly forbidden in the SL model and may induce stronger intermittency at small scales. However, $\beta > 1$ has never been reported in any type of turbulence. In this investigation, we applied the SL94 model in a newly observed microelectrokinetic (micro-EK) turbulent flow.

The experiment is conducted in an EK micromixer driven by ac electric field [14–16]. The quasi-T-shape microfluidics channel is plotted schematically in Fig. 5(a). Two electric conductive side walls were used as electrodes. Two streams with a conductivity ratio of 5000:1 were separated by a plastic splitter plate and delivered into the microchannel by a syringe pump. An ac signal with 100 kHz and 20 Vp-p was applied to generate the EK turbulence. The velocity fluctuation was measured by laser induced fluorescence photobleaching anemometer [17].

The measurements were pursued at downstream position ($x^* = x/w_c \geq 0.7$) from the entrance where the micro-EK turbulent flow becomes more homogeneous and isotropic. Typical velocity fluctuations at different downstream positions of the micro-EK turbulent flow have been plotted in Fig. 5(b). Compared to the velocity fluctuations of unforced flow which behave like white noise, the velocity fluctuations at four different x^* of the micro-EK turbulent flow all exhibit less small-scale components, and behave like random signal accompanied with burstlike events.

In Fig. 6(a), the relations of $S_2(l)$, $S_3(l)$, and $S_6(l)$ with spatial scale l are plotted. The Kolmogorov self-similarity of velocity structure functions can be clearly found within inertial subrange. Compared to the width of inertial subrange evaluated from the velocity power spectrum by Wang *et al.* [15], which is more than a decade long, the ones estimated from Fig. 6(a) are slightly shorter. This is consistent with the investigation of Davidson and Krogstad [18] who found the width of inertial subrange from power spectra was always larger than that of velocity structure functions, since the higher-order (including second-order) velocity structure functions are poor filters and can be contaminated by enstrophy information.

The streamwise evolution of $S_2(l)$ is plotted in Fig. 6(b). The width of inertial subrange decreases slightly along streamwise position from $x^* = 0.77$ to 3.84. At $x^* = 3.84$, the width of inertial subrange is only half decade, accompanied with an increasingly departure of ξ_2 from 2/3 predicted by the classical Kolmogorov self-similarity law. The decreasing of the width of inertial subrange and ξ_2 can be attributed to the decreasing electric Rayleigh number ($\text{Ra}_{e,l_0} = 4\langle|\Delta\sigma(l_0)|\rangle\varepsilon E_W^2 l_0^2 / \langle\sigma\rangle\rho\nu D$, where $\langle|\Delta\sigma(l_0)|\rangle$ represents the increment of electric conductivity (σ), ε is the electric permittivity of fluid, E_W is the bulk electric field intensity, and D is the effective diffusivity of σ). As the continuous consumption of $\langle|\Delta\sigma(l_0)|\rangle$, the electric body force (EBF) is reduced, and accordingly, the kinetic energy injection by EBF is reduced [19,20]. In the meanwhile, the kinetic energy is continuously dissipated by viscosity. When the energy injection rate by EBF is smaller than the

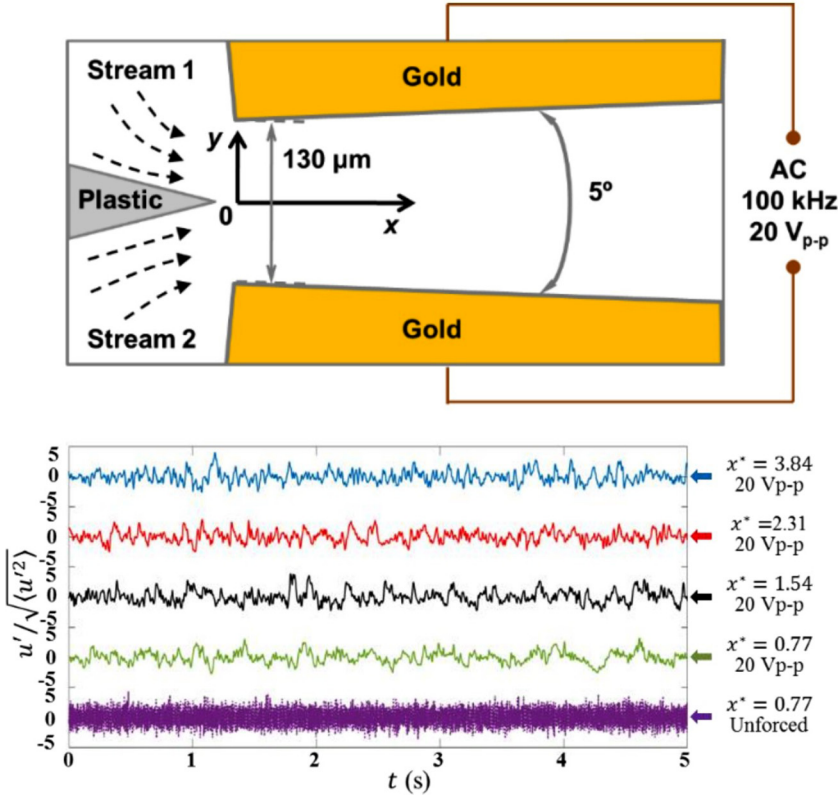


FIG. 5. Schematic of the microchip and time series of normalized velocity fluctuations $u'/\sqrt{\langle u'^2 \rangle}$. (a) Schematic of the microchannel for ac EK turbulence. Two streams have a conductivity ratio of 5000:1. The length (l_c), height (h) and initial width (w_c) of microchannel are 5 mm, 240 μm and 130 μm respectively. (b) Time series of normalized velocity fluctuations $u'/\sqrt{\langle u'^2 \rangle}$ at different x^* , where $u' = u - \langle u \rangle$.

dissipation rate, kinetic energy is mainly dissipated and only a small part of residual energy can form inertial subrange. This is why the width of inertial subrange continuously decreases with x^* .

It is interesting that the persistence time of turbulent state in this micro-EK turbulence is more than 0.15 s (calculated from $x^* = 0$ to 2.31), which is much larger than the lifetime of conventional hydrodynamic turbulence, e.g., in macroscale pipe flow, where the persistence time at this low Re (< 10 based on bulk flow velocity) is only 3×10^{-25} s [21,22]. In other words, if the turbulent state can be present in such low Re flow by hydrodynamics, it can only exist for 3×10^{-26} s which is much, much shorter than a spark. Therefore, the turbulent flow region we observed is only sustained because of the continuous injection of kinetic energy from EBF.

At $x^* = 0.77$ and 1.54, the intermittency evaluated by $\mu = 2 - \xi_6$ [1] is 0.48 and 0.38 respectively. Both of them are apparently larger than the 0.22 of high Re hydrodynamic turbulence [8]. The PDF of velocity increment should have larger deviation from Gaussian process. This can be clearly observed from Fig. 7. We selected the same three length scales, i.e., l_1 , l_2 , and l_3 , as marked in Fig. 6(b). The smaller the length scale, the stronger the deviation from Gaussian distribution, and the stronger the intermittency accordingly.

Nevertheless, in Fig. 7, P_l abnormally ascends at large $\Delta u(l)/[\Delta u(l)]_{rms}$ for length increment l_1 . These parts can significantly contribute to the intermittency of velocity structure functions. The flatness of velocity structure functions ($F_n = S_4(l)/S_2^2(l)$) varies between 3.9 and 3.3. The intermittency can be further evaluated by the intermittency factor β of hierarchical structures, which

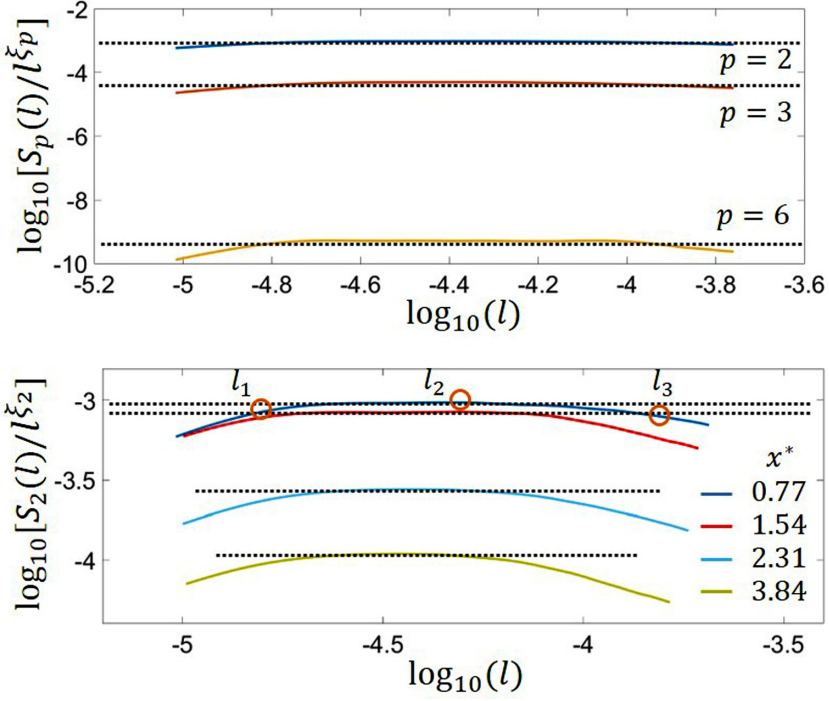


FIG. 6. Scaling behavior of velocity structure function. (a) $S_p(l)$ vs l at $x^* = 0.77$, where ξ_p are 0.68, 1.01 and 1.62 for $p = 2, 3$, and 6, respectively; (b) $S_2(l)$ vs l at four different x^* positions, where ξ_2 are 0.68, 0.69, 0.65, and 0.62 as x^* increases from 0.77 to 3.84.

is the focus of our concern. It is calculated by β test for each p and m , as [23,24]

$$H_{p+1, m+1}(l) = H_{p, m}(l)^{\beta(p, m)}, \quad (12)$$

where $H_{p, m}(l) = \frac{F_p(l) F_m(l_0)}{F_m(l) F_p(l_0)}$ and $F_p(l) = S_{p+1}(l)/S_p(l)$. l_0 is a reference scale which is the upper limit of inertial subrange. By linearly fitting the $\ln H_{p+1, m+1} \sim \ln H_{p, m}$ curve under each p , the corresponding exponent $\beta(p, m)$ can be simply calculated.

In Fig. 8, the curves of $\ln H_{p+1, m+1} \sim \ln H_{p, m}$ under different p and m are plotted. Generally speaking, all the plots show approximately linear relationships between $\ln H_{p+1, m+1}$ and $\ln H_{p, m}$,

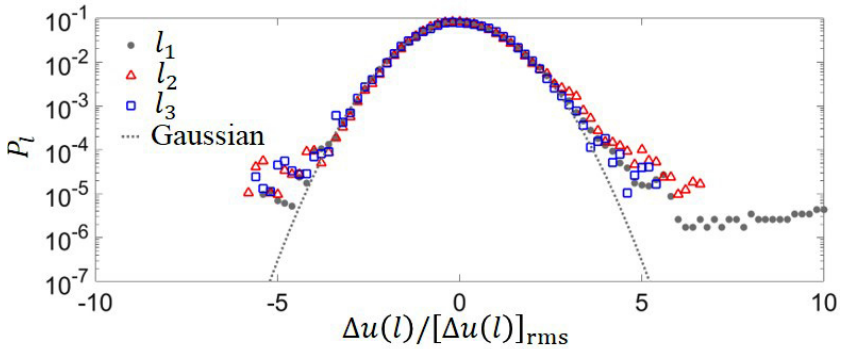


FIG. 7. P_l of different l at $x^* = 0.77$. The length increment l_1 , l_2 and l_3 are plotted in Fig. 2(b).

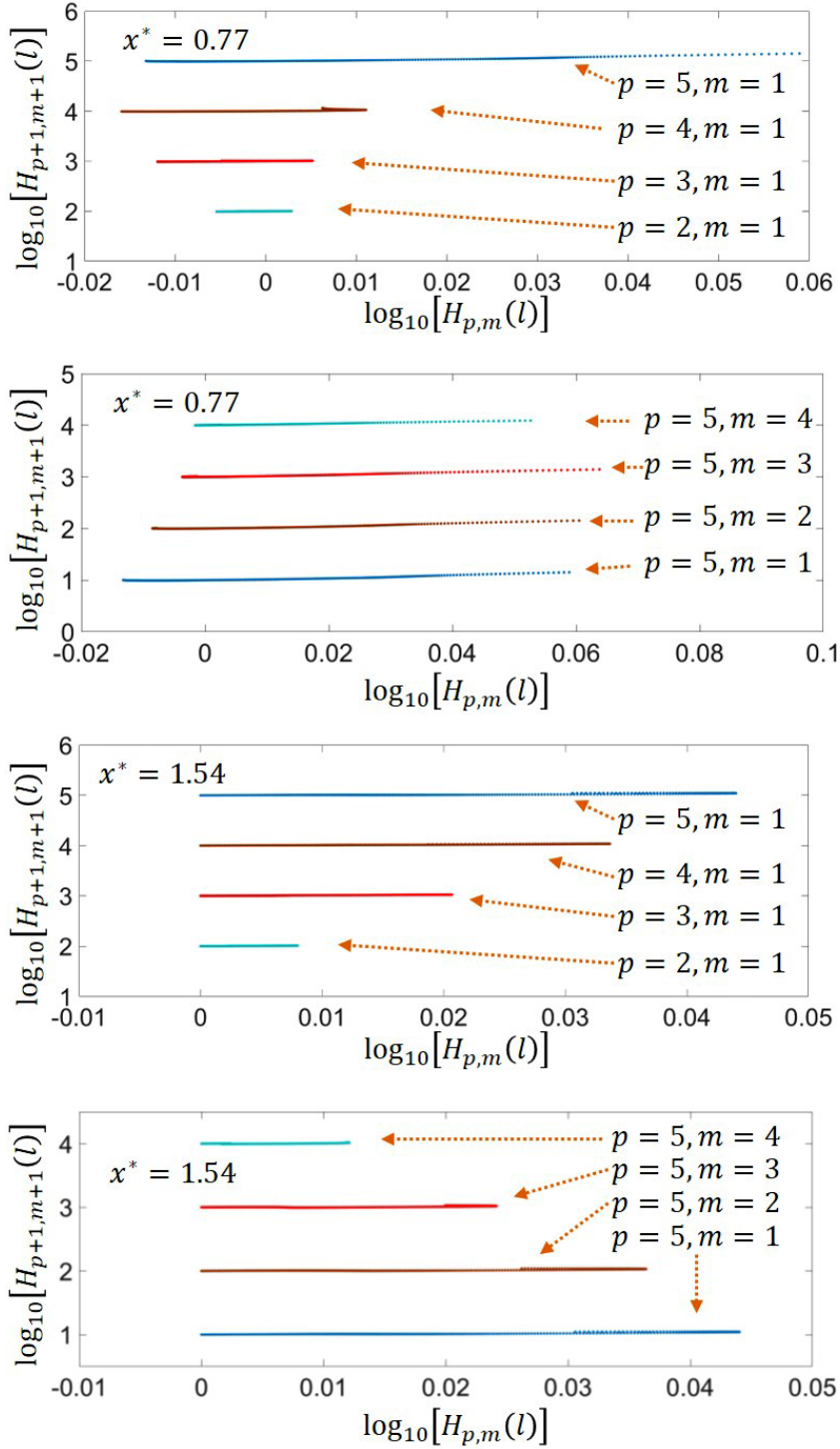


FIG. 8. $H_{p+1,m+1}(l)$ vs $H_{p,m}(l)$ for β -test. The slope of the curve is equal to β . (a), (b) at $x^* = 0.77$ and (c), (d) at $x^* = 1.54$. (a), (c) different p at $m = 1$, (b), (d) different m at $p = 5$.

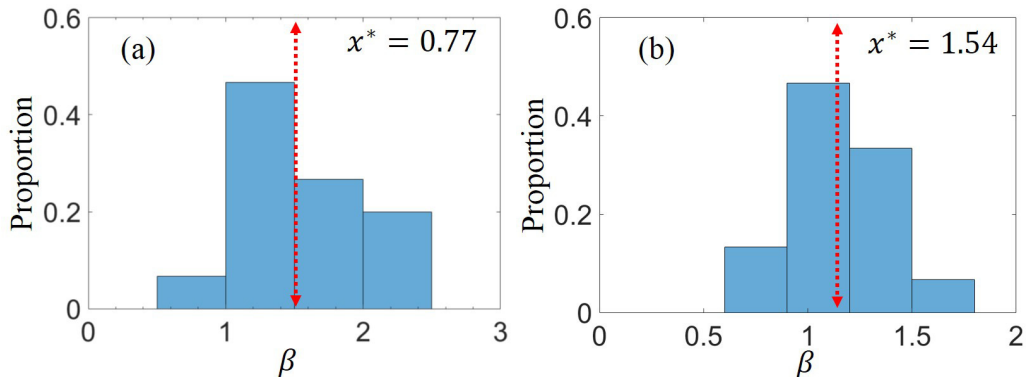


FIG. 9. Proportion of $\beta(p, m)$ calculated from Eq. (12) for all p and m . The red dashed line indicates β_{avg} at (a) $x^* = 0.77$ and (b) $x^* = 1.54$ respectively. The former has $\beta_{\text{avg}} = 1.51$ and latter has $\beta_{\text{avg}} = 1.13$.

which indicate the similarity of hierarchical structures. The slopes, e.g., $\beta(5, 1)$ and $\beta(5, 4)$, are 1.8 and 1.76, respectively. We expand the calculation of β to all p and m at $x^* = 0.77$ and 1.54 where the inertial subrange is approximately a decade long. The statistical results of β is plotted in Fig. 9. It can be seen that almost all $\beta(p, m)$ is above 1, which supports the existence of $\beta > 1$ in turbulent flows. The overall averaged β , which is

$$\beta_{\text{avg}} = \frac{1}{MN} \sum_{p=1}^N \sum_{m=1}^M \beta(p, m), \quad (13)$$

are 1.51 and 1.13 at $x^* = 0.77$ and 1.54 separately. Their influence on the PDF of velocity increment can be inferred from Fig. 4(a) and (b) respectively. Besides, decreasing of β_{avg} with x^* implies the decreasing of intermittency along the streamwise direction.

IV. DISCUSSIONS

$\beta > 1$ indicates a stronger relationship between P_l and P_{l_0} , compared to the conventional hydrodynamic turbulence, turbulent thermal convection and even MHD. As have been shown above, when $\beta > 1$, even a low intermittency PDF of velocity increment at large scale l_0 can induce a larger intermittency of PDF of velocity increment at smaller scale l , with much higher probability of large velocity increment. These findings are qualitatively consistent with the recent theoretical [19,20] and experimental investigations (on the PDF of velocity gradient) in EK turbulence [15]. Zhao and Wang [19,20] show that the scaling subrange controlled by EBF locates on the smaller scale side of inertial subrange, if two subranges coexist. Although the scalar field (e.g., electric conductivity) experiences direct cascade, the turbulent kinetic energy experiences a coexistence of direct and inverse cascades. EBF relies on electric conductivity gradient, it injects kinetic energy on small scales (relevant to electric conductivity gradient) and causes inverse cascade to form inertial subrange. In the meanwhile, the initially 2D interface of electric conductivity [19,20] is disturbed and forms fractal 3D interfaces after mixing. Electric conductivity gradients also exist on large scales, where EBF is induced and disturbs the flow field on large scales accordingly. Then, this part of turbulent kinetic energy cascades from large to small scales and contributes to the formation of inertial subrange. The coexistence of both direct and inverse cascades could be the reason for stronger relationship between P_l and P_{l_0} . When l approaches l_{ek} (a critical length scale between the inertial subrange and the EBF dominant subrange) [19,20] from inertial subrange, the velocity fluctuations could be inevitably affected by the EBF, which contributes to the deviation of P_l from Gaussian distribution, and in turn, leads to stronger intermittency. The finding of $\beta > 1$ in this

investigation supports the conjecture of Dubrulle [10] that the conservation laws dominate the value of β .

From SL94 model, if $\beta > 1$, the most singular dissipation structures could not be necessarily bound at very small scales. Nevertheless, since the existence of SL94 law is limited to inertial subrange, the truncation of $l \sim l_{ek}$ prevents the unbound event from being present. Also, by combining Eqs. (1) and (12) and let $m = p-1$, it is simply seen that

$$\beta = \frac{\xi_{p+2} + \xi_p - 2\xi_{p+1}}{\xi_{p+1} + \xi_{p-1} - 2\xi_p}. \quad (14)$$

After Taylor expansion on ξ_{p+q} according to the subscript, $\xi_{p+q} \approx \xi_p + q\xi'_p + \frac{q^2}{2!}\xi''_p + \frac{q^3}{3!}\xi'''_p + O(q^4)$, where $\xi'_p = d\xi_p/dp$ and so forth. By applying the result in Eq. (14), β can be expressed alternatively as $\beta \approx 1 + \xi'''_p/\xi''_p$. Apparently, the geometrical factor ξ'''_p/ξ''_p determines whether β is smaller or larger than unity. In conventional cases, ξ'''_p/ξ''_p is a negative constant along with p , and thus, the constant $\beta < 1$. In EK turbulence, ξ'''_p/ξ''_p exhibits positive values. Furthermore, ξ'''_p/ξ''_p is sensitive to the quantity of experimental data under large p . Although the data in this investigation is sufficient to calculate ξ_p up to $p = 6$, the calculated β exhibits scattering around its averaged value, as can be seen from Fig. 9.

V. CONCLUSIONS

In the present work, the intermittency of a typical ac EK turbulence is investigated based on the scaling exponent function ξ_p of velocity structure functions according to the SL94 model. Remarkably, $\beta > 1$ was experimentally observed in electrokinetic turbulence. We theoretically analyzed the probable influence if $\beta > 1$. It is found that when $0 < \beta \leq 1$, the probability density function of velocity increment at small scale l is only determined by $P_{l_0, >}[\Delta u(l_0)]$ on large scale l_0 . When $\beta > 1$, the probability density function of velocity increment at small scale l can be determined by both $P_{l_0, >}[\Delta u(l_0)]$ and $P_{l_0, <}[\Delta u(l_0)]$, which makes a significant contribution to the intermittency of turbulence. A strong intermittency can be predicted from $\beta > 1$, and accompanied by the probability density function of velocity increment at small scale l , which exhibits abnormally ascending from Gaussian distribution at large $\Delta u(l)$.

This study provides insight into the cause of intermittency in micro-EK turbulence. The result $\beta > 1$ implies there exists a new route to turbulence, through a different but tighter relationship between large and small scale velocity structures. It is also inspiring for studying other turbulence in an open system, where energy infill is directly executed in a wide subrange of wavelengths.

ACKNOWLEDGMENTS

For this research work, W.Z. was supported by the National Natural Science Foundation of China (Grant No. 11672229), G.W. was supported by NSF CAREER Grants No. CBET-0954977 and No. CBET-1336004 of the United States.

-
- [1] U. Frisch, *Turbulence—The Legacy of A. N. Kolmogorov* (Cambridge University Press, New York, USA, 1995).
 - [2] A. N. Kolmogorov, The local structure of turbulence in incompressible viscous fluid for very large Reynolds numbers, *Dokl. Akad. Nauk SSSR* **30**, 301 (1941).
 - [3] A. N. Kolmogorov, A refinement of previous hypotheses concerning the local structure of turbulence in a viscous incompressible fluid at high Reynolds number, *J. Fluid Mech.* **13**, 82 (1962).
 - [4] Z.-S. She and E. C. Waymire, Quantized Energy Cascade and Log-Poisson Statistics in Fully Developed Turbulence, *Phys. Rev. Lett.* **74**, 262 (1995).

- [5] Z.-S. She and E. Leveque, Universal Scaling Laws in Fully Developed Turbulence, [Phys. Rev. Lett. **72**, 336 \(1994\)](#).
- [6] G. R. Chavarria, C. Baudet, R. Benzi, and S. Ciliberto, Hierarchy of the velocity structure functions in fully developed turbulence, [J. Phys. II France **5**, 485 \(1995\)](#).
- [7] G. R. Chavarria, C. Baudet, and S. Ciliberto, Hierarchy of the TED Moments in Fully Developed Turbulence, [Phys. Rev. Lett. **74**, 1986 \(1995\)](#).
- [8] R. Benzi, L. Biferale, S. Ciliberto, M. V. Struglia, and R. Tripicciono, Generalized scaling in fully developed turbulence, [Physica D **96**, 162 \(1996\)](#).
- [9] H. Politano and A. Pouquet, Model of intermittency in magnetohydrodynamic turbulence, [Phys. Rev. E **52**, 636 \(1995\)](#).
- [10] B. Dubrulle, Intermittency in Fully Developed Turbulence: Log-Poisson Statistics and Generalized Scale Covariance, [Phys. Rev. Lett. **73**, 959 \(1994\)](#).
- [11] R. Camussi and R. Benzi, Hierarchy of transverse structure functions, [Phys. Fluids **9**, 257 \(1997\)](#).
- [12] E. Leveque, G. Ruiz-Chavarria, C. Baudet, and S. Ciliberto, Scaling laws for the turbulent mixing of a passive scalar in the wake of a cylinder, [Phys. Fluids **11**, 1869 \(1999\)](#).
- [13] Z.-S. She and W.-D. Su, in *The Latest Advances in Turbulent Researches (in Chinese)*, edited by J.-J. Wang *et al.* (Science Publishing Company Press, Beijing, 2001), p. 1.
- [14] G. Wang, F. Yang, and W. Zhao, There can be turbulence in microfluidics at low Reynolds number, [Lab Chip **14**, 1452 \(2014\)](#).
- [15] G. Wang, F. Yang, and W. Zhao, Micro electrokinetic turbulence in microfluidics at low Reynolds number, [Phys. Rev. E **93**, 013106 \(2016\)](#).
- [16] G. Wang, F. Yang, W. Zhao, and C.-P. Chen, On micro-electrokinetic scalar turbulence in microfluidics at low Reynolds number, [Lab Chip **16**, 1030 \(2016\)](#).
- [17] W. Zhao, F. Yang, J. Khan, K. Reifsnider, and G. Wang, Measurement of velocity fluctuations in microfluidics with simultaneously ultrahigh spatial and temporal resolution, [Exp. Fluids **57**, 11 \(2016\)](#).
- [18] P. A. Davidson and P.-Å. Krogstad, On the deficiency of even-order structure functions as inertial-range diagnostics, [J. Fluid Mech. **602**, 287 \(2008\)](#).
- [19] W. Zhao and G. Wang, Scaling of velocity and scalar structure functions in ac electrokinetic turbulence, [Phys. Rev. E **95**, 023111 \(2017\)](#).
- [20] W. Zhao and G. Wang, Cascade of turbulent energy and scalar variance in DC electrokinetic turbulence, [Physica D **399**, 42 \(2019\)](#).
- [21] B. Hof, J. Westerweel, T. M. Schneider, and B. Eckhardt, Finite lifetime of turbulence in shear flows, [Nature \(London\) **443**, 59 \(2006\)](#).
- [22] B. Eckhardt, T. M. Schneider, B. Hof, and J. Westerweel, Turbulence Transition in Pipe Flow, [Annu. Rev. Fluid Mech. **39**, 447 \(2007\)](#).
- [23] Z.-S. She, K. Ren, G. S. Lewis, and H. L. Swinney, Scalings and structures in turbulent Couette-Taylor flow, [Phys. Rev. E **64**, 016308 \(2001\)](#).
- [24] Z. Zou, Y. Zhu, M. Zhou, and Z.-S. She, Hierarchical structures in a turbulent pipe flow, [Fluid Dyn. Res. **33**, 493 \(2003\)](#).